

Diffusion Effects in Gradient Echo Memory

X.-W. Luo^{1,2}, J. J. Hope³, B. Hillman³, and T. M. Stace^{1*}

¹*ARC Centre for Engineered Quantum Systems, University of Queensland, St Lucia, QLD 4072, Australia*

²*Key Lab of Quantum Information, CAS, University of Science and Technology of China, Hefei, Anhui, 230026, P.R. China and*

³*Department of Quantum Science, Research School of Physics and Engineering, The Australian National University, Canberra, ACT0200, Australia*

We study the effects of diffusion on a Λ -gradient echo memory, which is a coherent optical quantum memory using thermal gases. The efficiency of this memory is high for short storage time, but decreases exponentially due to decoherence as the storage time is increased. We study the effects of both longitudinal and transverse diffusion in this memory system, and give both analytical and numerical results that are in good agreement. Our results show that diffusion has a significant effect on the efficiency. Further, we suggest ways to reduce these effects to improve storage efficiency.

I. INTRODUCTION

Quantum memory is an important tool in many quantum information protocols, including quantum repeaters for long-distance quantum communication [1], and identity quantum gates in quantum computation [2]. Numerous optical quantum memories have been developed, including electromagnetically-induced transparency (EIT) based quantum memory [3, 4], far-detuned Raman process memory [5, 6], and photon-echo quantum memories: controlled reversible inhomogeneous broadening (CRIB) memory [7, 8], atomic frequency combs (AFC) memory [9], and gradient echo memory (GEM) [10–12]. A review of these schemes can be found in [13]. Of these schemes, the most impressive efficiency so far attained experimentally is 87% by Λ -GEM scheme [14] using warm rubidium vapor. In this paper, we will examine the effects of atomic diffusion on the Λ -GEM system, which may limit this efficiency for larger storage times.

Λ -GEM is a memory using a 3-level, Λ -type atom (Fig. 1). The input optical pulse couples the two metastable lower states through a control field. The excited state is coupled in the far detuned region, so the 3-level atoms can be treated as effective 2-level atoms. These effective two-level atoms have linearly increasing atomic Zeeman shifts along the length of the storage medium. The pulse is first absorbed, then by simply reversing the sign of the magnetic field, the pulse is retrieved in the forward direction. The incident signal field is converted to a collective atomic excitation known as a spin wave, which is distributed as a function of position. The Brownian motion of the gaseous atoms will cause diffusion, which will disturb spatial coherence of the atomic spin-wave, leading to decoherence. For a plane wave, only axial diffusion is important, but transverse diffusion becomes significant when a realistic beam profile is included. There has been recent interest in the effects of diffusion in the EIT [15–17]. In this work, we study the effects of diffusion in Λ -GEM system, giving analytical and numerical results.

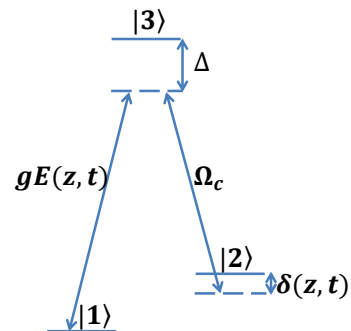


FIG. 1. Level structure of Λ -type 3-level atom.

We also suggest ways to reduce these effects to improve storage efficiency.

II. Λ GRADIENT ECHO MEMORY

We consider a medium consisting of Λ -type 3-level atoms with two metastable lower states as shown in Fig. 1. The ground state $|1\rangle$ and the excited state $|3\rangle$ are coupled by a weak optical field, the positive frequency component of the electric field is described by the slowly varying operator

$$\hat{E}(\mathbf{r}, t) = \sum_{\mathbf{k}} \sqrt{\frac{1}{V}} a_{\mathbf{k}}(t) e^{i\mathbf{k}\cdot\mathbf{r}} e^{-ik_0 z} e^{i\omega_0 t} \quad (1)$$

with detuning Δ , where V is the quantization volume, ω_0 is the carrier frequency of the quantum field and $k_0 = \omega_0/c$. The excited state $|3\rangle$ is also coupled to the metastable state $|2\rangle$ via a coherent control field with Rabi frequency Ω_c and a two photon detuning δ . This two photon detuning is spatially varied $\delta(z, t) = \eta(t)z$, with time dependent gradient $\eta(t)$. Then the interaction Hamiltonian in the rotating frame with respect to the field

* stace@physics.uq.edu.au

frequencies is

$$\hat{H} = \sum_n [\hbar\Delta\sigma_{33}^{(n)} + \hbar\delta(z_n, t)\sigma_{22}^{(n)} + \hbar\sum_{\mathbf{k}} (\hbar g_{\mathbf{k}} a_{\mathbf{k}} e^{i\mathbf{k}\cdot\mathbf{r}_n} \sigma_{31}^{(n)} + \hbar\Omega_c(\mathbf{r}_n)\sigma_{32}^{(n)} + h.c)], \quad (2)$$

where $g_{\mathbf{k}} = \wp\sqrt{\frac{\omega_{\mathbf{k}}}{2\hbar\epsilon_0 V}}$ is the atom-field coupling constant with \wp being the dipole moment of the 1-3 transition, and $\sigma_{\mu\nu}^{(n)} = |\mu\rangle_n\langle\nu|$ is an operator acting on the n -th atom at $\mathbf{r}_n = (x_n, y_n, z_n)$. We assume that initially all atoms are in their ground state $|1\rangle$. We transform to collective operators, which are averages over atomic operators over a small volume centered at \mathbf{r} containing $N_r \gg 1$ particles,

$$\sigma_{\mu\nu}(\mathbf{r}, t) = \frac{1}{N_r} \sum_{j=1}^{N_r} \sigma_{\mu\nu}^{(j)}(t) \quad (3)$$

From the Heisenberg-Langevin equations in the weak probe region ($\sigma_{11} \simeq 1, \sigma_{22} \simeq \sigma_{33} \simeq 0$), we get the Maxwell-Bloch equations [18],

$$\begin{aligned} \dot{\sigma}_{13}^{(n)} &= -(\gamma_{13} + i\Delta)\sigma_{13}^{(n)} + ig e^{ik_0 z_n} E(\mathbf{r}_n, t) + i\Omega_c e^{ik_c z_n} \sigma_{12}^{(n)}, \\ \dot{\sigma}_{12}^{(n)} &= -(\gamma_{12} + i\delta(z_n, t))\sigma_{12}^{(n)} + i\Omega_c e^{-ik_c z_n} \sigma_{13}^{(n)}, \\ \left(\frac{\partial}{\partial t} + c\frac{\partial}{\partial z} - ic\frac{\nabla_x^2 + \nabla_y^2}{2k_0}\right) E(\mathbf{r}, t) &= igN e^{-ik_0 z} \sigma_{13}(\mathbf{r}, t), \end{aligned} \quad (4)$$

where $\gamma_{\nu\mu}$ are the decay rates, $g = \wp\sqrt{\frac{\omega_0}{2\hbar\epsilon_0}}$, and N is the atomic density. We have assumed that $g_{\mathbf{k}} \simeq \wp\sqrt{\frac{\omega_0}{2\hbar\epsilon_0 V}}$ and $\Omega_c(\mathbf{r}) = \Omega_c e^{ik_c z}$. We also omit the Langevin noise operators since here we are more interested in the decoherence caused by diffusion. This is equivalent to making a semiclassical approximation for the electric field and the atomic coherences.

In Eq. (4), $ic\frac{\nabla_x^2 + \nabla_y^2}{2k_0}$ is the diffraction term, and generally, the diffraction effects can be neglected [19]. Notice that we are here considering the regime $t_p \gg L/c$, where $2t_p$ is the temporal width of the signal, and $2L$ is the length of the medium. This allows us to neglect temporal retardation effects, i.e., we can neglect the temporal derivative in the third equation of Eq. (4). Also, since the atoms are far detuned ($\Delta \gg \gamma_{13}, \Omega_c$), we adiabatically eliminate the fast oscillations and set $\dot{\sigma}_{13}^{(n)} = 0$. Then we have $\sigma_{13} = (g e^{ik_0 z} E + \Omega_c e^{ik_c z} \sigma_{12})/\Delta$, and we get the reduced Maxwell-Bloch equations,

$$\begin{aligned} \dot{\sigma}_{12}^{(n)} &= -(i\delta(z_n, t) - i\frac{\Omega_c^2}{\Delta})\sigma_{12}^{(n)} \\ &\quad + i\frac{g\Omega_c}{\Delta} e^{i(k_0 - k_c)z_n} E(\mathbf{r}_n, t), \\ \frac{\partial}{\partial z} E(\mathbf{r}, t) &= i\frac{gN\Omega_c}{c\Delta} e^{-i(k_0 - k_c)z} \sigma_{12}(\mathbf{r}, t) \\ &\quad + i\frac{g^2 N}{c\Delta} E(\mathbf{r}, t). \end{aligned} \quad (5)$$

Here we neglect decay, i.e. $\gamma_{12} \rightarrow 0$, since we consider the storage time much less than $1/\gamma_{12}$.

III. DIFFUSION

We now consider the effects of diffusion on the atomic state. In order to isolate the motional effects of diffusion from collisional dephasing, we assume that the collisions between atoms do not change the state of the atom. Then we derive the diffusion equation for the atomic density matrix ρ . Space is divided into volume elements with length Δr and center r . We associate a density matrix $\rho(r, t)$ with atoms in this volume element, given by

$$\rho(r, t) = \frac{1}{N_r} \sum_{j=1}^{N_r} \rho^{(j)}(t),$$

where N_r is the atom number in volume centered at r . The total density matrix for the entire system is assumed to be the tensor product of these local density matrices.

Diffusion causes an exchange of atoms between adjacent volumes. During a short time Δt , a fraction ϵ of the atoms in slice r migrate into slice $r \pm \Delta r$. There is also atomic flux back into slice r from $r \pm \Delta r$. We assume that the total number density of the atoms is uniform, so the state at r and $t + \Delta t$ is described by the new density matrix which is the average of the density matrix of atoms remaining in the volume and those that have migrated in to it. The diffusive component of the evolution is therefore

$$\begin{aligned} \rho(r, t + \Delta t) &= (1 - 2\epsilon)\rho(r, t) \\ &\quad + \epsilon(\rho(r + \Delta r, t) + \rho(r - \Delta r, t)) \\ \Rightarrow \partial_t \rho(r, t) &= D\nabla^2 \rho(r, t) \end{aligned} \quad (6)$$

where $D = \epsilon\Delta r^2/\Delta t$ is the diffusion coefficient. With the same consideration, we get the diffusive component evolution for the atomic correlation functions

$$\dot{\sigma}_{\mu\nu}(r, t) = D\nabla^2 \sigma_{\mu\nu}(r, t) \quad (7)$$

Now we introduce the interaction with optical fields. Since diffusion is caused by Brownian motion, this will lead to Doppler shifts in the various detunings. We now consider the interaction between the optical field and a single atom, and quantify the effects of these Doppler shifts. The atom moves at some random velocity, and there will be a Doppler shift for both the signal and control fields. So the detunings in Eq. (4) become $\Delta = \Delta_0 + \Delta_{Dopp}$, and $\delta = \delta_0 + \delta_{Dopp}$, with Δ_0, δ_0 the detunings for stationary atoms and $\Delta_{Dopp}, \delta_{Dopp}$ the Doppler shifts. Typically, the one photon Doppler shift $\Delta_{Dopp} \ll \Delta_0$, state $|3\rangle$ is still far detuned. So the adiabatic elimination is still valid in the presence of the Brownian motion induced Doppler shift, and we can still reduce the 3-level atom to an effective 2-level atom. The Maxwell-Bloch equation will still reduce to Eq. (5), but

with one photon detuning $\Delta = \Delta_0 + \Delta_{Dopp}$ and two photon detuning $\delta = \delta_0 + \delta_{Dopp}$. So, for the reduced two level atomic system, the diffusive Maxwell-Bloch equation for the collective correlation $\sigma_{12}(z, t)$ averaged over atoms in each volume is

$$\begin{aligned} \dot{\sigma}_{12}(\mathbf{r}, t) &= i \frac{g\Omega_c}{\Delta} e^{i(k_0 - k_c)z} E(\mathbf{r}, t) \\ &\quad - i\delta(z, t)\sigma_{12}(\mathbf{r}, t) + D\nabla^2\sigma_{12}(\mathbf{r}, t), \\ \frac{\partial}{\partial z} E(\mathbf{r}, t) &= i \frac{gN\Omega_c}{c\Delta} e^{-i(k_0 - k_c)z} \sigma_{12}(\mathbf{r}, t) \\ &\quad + i \frac{g^2N}{c\Delta} E(\mathbf{r}, t). \end{aligned} \quad (8)$$

We have absorbed the Stark shift $\frac{\Omega_c^2}{\Delta}$ into the two-photon detuning. Here our diffusive Maxwell-Bloch equation is consistent with the result in the EIT system [15, 17].

Notice that the signal and control fields are co-propagating, so the Doppler broadening width for δ is typically 1kHz, which is much smaller than the frequency width of the signal field (~ 1 MHz), so we neglect this two-photon Doppler broadening δ_{Dopp} and replace $\delta(z, t)$ by $\delta_0(z, t) = \eta(t)z, z \in [-L, L]$.

For the one photon detuning $\Delta = \Delta_0 + \Delta_{Dopp}$, after we make the adiabatic elimination, it will appear in the denominator (see Eq. (8)), so

$$\frac{1}{\Delta} \simeq \frac{1}{\Delta_0} \left(1 - \frac{\Delta_{Dopp}}{\Delta_0} + \left(\frac{\Delta_{Dopp}}{\Delta_0} \right)^2 \right).$$

The term linear in Δ_{Dopp} will vanish when we average over many atoms in a volume centred at r , so we can replace Δ by Δ_0 in our Maxwell-Bloch equation, with second order accuracy [typically $(\Delta_{Dopp}/\Delta_0)^2 \sim 10^{-3}$].

IV. ANALYTIC CALCULATION AND NUMERICAL SIMULATION

To quantify the effects of diffusion, we solve for the atomic dynamics. There are three distinct phases during the storage: write-in $-t_0 < t < 0$, during which the signal is absorbed by the memory; hold $0 < t < t_H$, during which the information is stored in the memory and the gradient is turned off; read-out $t_H < t < t_H + t_0$, during which the signal is emitted by turning on the flipped gradient.

We quantify the effects of diffusion by the read-out efficiency ε defined to be

$$\varepsilon = \frac{\int_{t_H}^{t_H+t_0} |f_{out}(t)|^2 dt}{\int_{-t_0}^0 |f_{in}(t)|^2 dt} \quad (9)$$

where $f_{out}(t) = E(z = L, t > t_H)$ is the output field and $f_{in}(t) = E(z = -L, t < 0)$ is the input field. We solve for $f_{out}(t)$ both numerically and analytically, and consider the effects of diffusion in axial (longitude) and radial (transverse) directions separately.

A. Longitudinal diffusion

For a uniform plane wave, transverse diffusion is irrelevant. We replace \mathbf{r} by z in Eq. (8) and consider the longitude diffusion in a 1-dimensional model. Now the Maxwell-Bloch equation is

$$\begin{aligned} \dot{\sigma}_{12}(z, t) &= i \frac{g\Omega_c}{\Delta} e^{i(k_0 - k_c)z} E(z, t) \\ &\quad - i\delta(z, t)\sigma_{12}(z, t) + D\nabla_z^2\sigma_{12}(z, t), \\ \frac{\partial}{\partial z} E(z, t) &= i \frac{gN\Omega_c}{c\Delta} e^{-i(k_0 - k_c)z} \sigma_{12}(z, t) \\ &\quad + i \frac{g^2N}{c\Delta} E(z, t). \end{aligned} \quad (10)$$

We now investigate the longitude diffusion effects during the write-in process, the hold time and the read-out processes separately.

To compute $f_{out}(t)$, we evolve Eq. (10) using η as in Fig. 5 (a). Following the method given in [10], we first propagate $E(z, t)$ and $\sigma_{12}(z, t)$ forward with boundary condition $E(z = -L, t < 0) = f_{in}(t)$ to find their values at time t_H . Then we propagate E and σ_{12} backward to time t_H , with final condition $E(z = L, t > t_H) = f_{out}(t)$, and solve for $f_{out}(t)$ by matching the two solutions at time t_H .

Write: Consider the diffusion effects during the write-in process, we find that (see Appendix A)

$$f_{out}(t_H + t) = e^{\frac{-D}{3\eta}(k_i^3 - (k_i - \eta t)^3)} f_{in}(-t) \bar{G} \quad (11)$$

where $k_i = \frac{g^2N}{c\Delta} + k_0 - k_c - \frac{\beta}{L}$ is the initial spatial frequency of $\sigma_{12}(z, t)$, and

$$\bar{G} = |\eta L \left(t + \frac{\beta}{\eta L} \right) |^{-i2\beta} e^{i\frac{2Lg^2N}{c\Delta}} e^{-i\frac{g_{eff}^2N}{c\eta(t + \frac{\beta}{\eta L})} t_H} \Gamma(i\beta)/\Gamma(-i\beta)$$

is a phase factor, with $g_{eff} = g\Omega_c/\Delta$ and $\beta = \frac{g_{eff}^2N}{\eta c}$. For a pulse with Gaussian temporal profile $f_{in} = Ae^{-(t+t_{in})^2/t_p^2}$, we find

$$\varepsilon_W = \frac{\int_{-t_0}^0 dt e^{-2(t+t_{in})^2/t_p^2} e^{\frac{-2D}{3\eta}(k_i^3 - (k_i + \eta t)^3)}}{\int_{-t_0}^0 dt e^{-2(t+t_{in})^2/t_p^2}}. \quad (12)$$

Typically, $D\eta^2 t_p^3$ is very small, then the efficiency is

$$\varepsilon_W = \sqrt{\alpha_W} e^{-\tau_W} + O(D^2 \eta^4 t_p^6) \quad (13)$$

where $\alpha_W = \frac{1}{1 - D\eta^2 t_p^2 (k_i/\eta - t_{in})}$ and $\tau_W = \frac{2D\eta^2}{3} \left[\left(\frac{k_i}{\eta} \right)^3 - \left(\frac{k_i}{\eta} - t_{in} \right)^3 \right]$ are dimensionless parameters. For typical experimental parameters, $\alpha_W \simeq 1$, then

$$\varepsilon_W \simeq e^{-\tau_W} \quad (14)$$

We also numerically solve Eq. (10) with diffusion during the write-in process, using XMDS [20]. We calculate the efficiency for different values of the diffusion rate D , input time t_{in} etc. The results are shown in Fig. 2, (points are numerical results, and the curve is Eq. (14)). We plot the efficiency ε_W with respect to the rescaled dimensionless parameter τ_W , so all the points with different parameters collapse on a single curve.

Hold: During the storage time $[0, t_H]$, we find (see Appendix A)

$$f_{out}(t_H + t) = e^{-Dt_H(k_i - \eta t)^2} f_{in}(-t) \bar{G} \quad (15)$$

For the above Gaussian shape input, the efficiency is given by

$$\varepsilon_H = \sqrt{\alpha_H} e^{-2\alpha_H \tau_H}, \quad (16)$$

where $\alpha_H = \frac{1}{t_p^2} / \left(\frac{1}{t_p^2} + Dt_H \eta^2 \right)$ and $\tau_H = Dt_H k_H^2$ are dimensionless parameters, with $k_H = k_i - \eta t_{in}$. For typical experimental parameters, $\alpha_H \simeq 1$ and we have

$$\varepsilon_H \simeq e^{-2\tau_H}. \quad (17)$$

We also numerically solve Eq. (10) with diffusion during hold time, using XMDS. We calculate the efficiency for different values of the diffusion rate D , storage time t_H etc. The results are shown in Fig. 3 (points are numerical results, and curve is Eq. (17)). We plot the efficiency ε_H with respect to the rescaled dimensionless parameter τ_H , so all the points with different parameters collapse on a single curve.

Read: the diffusion effects during the read-out process are the same as the diffusion effects of the write-in process (see the appendix A), so we simply have

$$\varepsilon_R = \varepsilon_W.$$

B. Transverse diffusion

We now quantify the effects of diffusion for a beam with realistic transverse Gaussian profile. The efficiency for a 3-dimensional model is defined as

$$\varepsilon = \frac{\int |f_{out}(x, y, t_H + t)|^2 dx dy dt}{\int |f_{in}(x, y, t)|^2 dx dy dt} \quad (18)$$

Eq. (8) can be solved in Fourier space k_x, k_y , and also notice that

$$\varepsilon = \frac{\int |f_{out}(k_x, k_y, t_H + t)|^2 dk_x dk_y dt}{\int |f_{in}(k_x, k_y, t)|^2 dk_x dk_y dt} \quad (19)$$

Eq. (8) can be reduced to a quasi-1D problem, and can be solved as before (see Appendix B). For transverse diffusion, the output pulse will be

$$f_{out}(k_x, k_y, t_H + t) = e^{-2\gamma_k t} e^{-\gamma_k t_H} f_{in}(k_x, k_y, -t) \bar{G}. \quad (20)$$

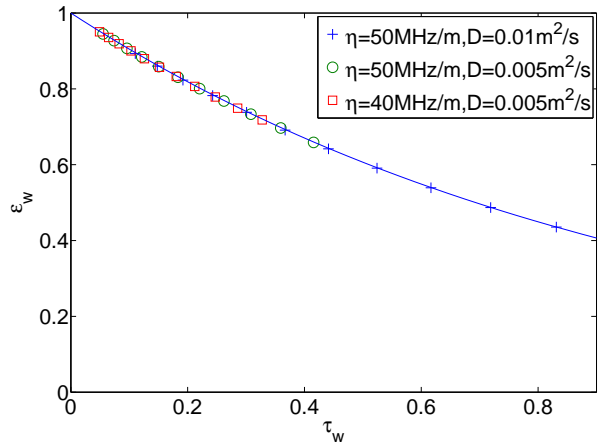


FIG. 2. The efficiency decay with respect to the dimensionless parameter τ_W for longitude diffusion during the write-in time, the points are numerical results, and the curve is Eq. (14).

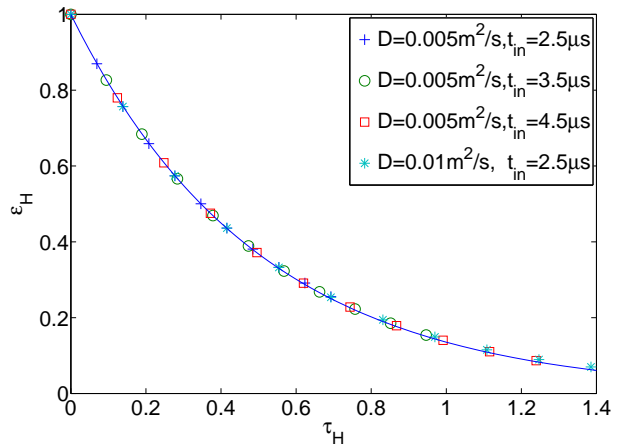


FIG. 3. The efficiency decay with respect to the dimensionless parameter τ_H for longitude diffusion during hold time, the points are numerical results, and the curve is Eq. (17).

where $\gamma_k = D(k_x^2 + k_y^2)$.

If the input pulse has both Gaussian temporal and transverse profile,

$$f_{in}(x, y, t) = A e^{-(x^2+y^2)/a^2} e^{-(t+t_{in})^2/t_p^2},$$

then $\gamma_k t_p \sim Dt_p/a^2$, which is typically small. Thus the memory efficiency is

$$\varepsilon_{\perp} = \frac{1}{1 + \tau_{\perp}} + O(\gamma_k^2 t_p^2), \quad (21)$$

where $\tau_{\perp} = 4D(t_H + 2t_{in})/a^2$ is a dimensionless parameter.

We also numerically solve Eq. (8) with $\nabla^2 = \nabla_x^2 + \nabla_y^2$. We calculate the efficiency for different values of a, t_H etc. The results are shown in Fig. 4 (points are numerical results, and curve is Eq. (21)). We plot the efficiency ε_{\perp}

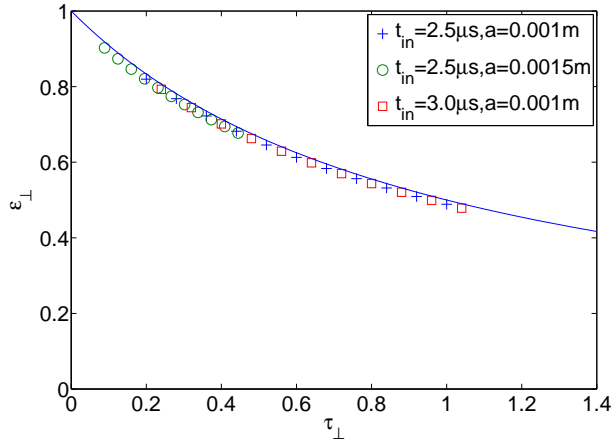


FIG. 4. Efficiency decay with respect to τ_{\perp} for transverse diffusion, the points are numerical results, and the curve is Eq. (21).

with respect to the rescaled dimensionless parameter τ_{\perp} , so all the points with different parameters collapse on a single curve.

C. Total diffusion

Experimentally, longitude and transverse diffusion coexist during the whole process. Combining all the diffusive contributions mentioned above, we get the output field as (Appendix B)

$$f_{out}(k_x, k_y, t_H + t) = e^{\frac{-2D}{3\eta}(k_i^3 - (k_i - \eta t)^3)} e^{-Dt_H(k_i - \eta t)^2} \times e^{-2\gamma_k t - \gamma_k t_H} f_{in}(k_x, k_y, -t) \bar{G}. \quad (22)$$

We consider input pulse with both Gaussian temporal and transverse profile as above, typically, $D\eta^2 t_p^3$, $\gamma_k t_p$ are very small. Then the total efficiency will be

$$\varepsilon_{tot} = \sqrt{\frac{1}{1/\alpha_H + 2/\alpha_W - 2}} e^{-2\tau_W} e^{-2\tau_H} \frac{1}{1 + \tau_{\perp}} + O[(D\eta^2 t_p^3, \gamma_k t_p)^2] \quad (23)$$

Typically, $\alpha_H \simeq 1$, $\alpha_W \simeq 1$, so we have

$$\varepsilon_{tot} \simeq \varepsilon_W \times \varepsilon_H \times \varepsilon_R \times \varepsilon_{\perp}.$$

D. Efficiency optimization and estimation

Our model did not examine other decoherence processes, such as control field-induced scattering and ground state decoherence. Our results simply quantify the effects of motional diffusion on GEM efficiency, and therefore the represent upper estimates for the performance of GEM.

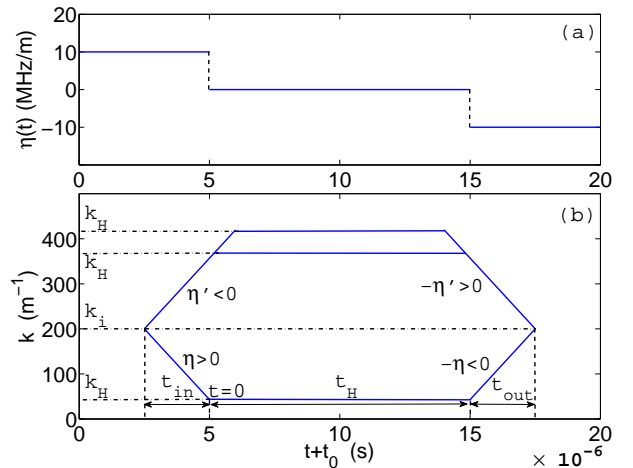


FIG. 5. (a) The gradient is turned off during hold time, and flipped for read-out. (b) An illustration of the spatial frequency for $\sigma_{12}(z, t)$, k decreases or increases depending on the sign of the gradient.

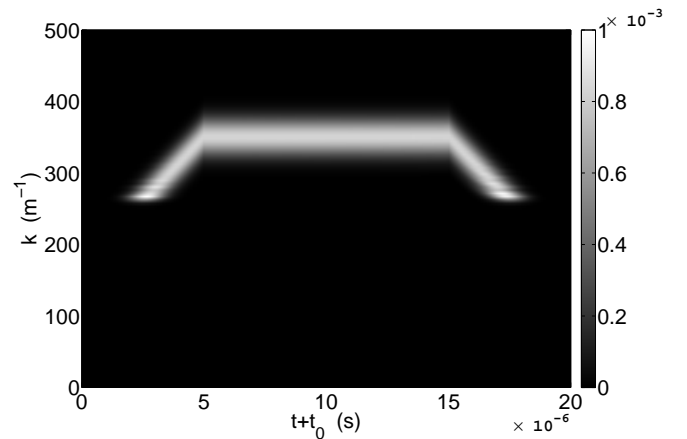


FIG. 6. Numerical results of $|\sigma_{12}(k, t)|$ with write-in gradient $\eta' < 0$.

Structures with larger spatial frequency will decay faster under diffusion. For the 1D model during hold time, we have (see the Appendix A)

$$\sigma_{12}(k, t) \propto f_{in}\left(\frac{k - k_i}{\eta}\right) \quad (24)$$

The input pulse is centered at $-t_{in}$, then we have $k \sim k_H = k_i - \eta t_{in}$. We see that k will increase or decrease as t_{in} increases, depending on the sign of η . During the hold time $[0, t_H]$, the gradient is turned off, and k will hold its value. The read-out process is symmetric to the write-in process (see fig. 5), returning the quasi-momentum to its original distribution. Fig. 6 shows the numerical result by solving Maxwell-Bloch equations.

One way to reduce the effects of diffusion is to remove the gradient during the storage part of the process, and only turn on the flipped gradient during readout. For

realistic t_{in} and η , we can get zero spatial frequency $k_H = 0$, for which $\tau_H = 0$, and this will minimise the diffusional decay rate. We then have $\varepsilon_H = \sqrt{\alpha}$ and $\varepsilon_W = e^{-2Dk_i^2 t_{in}/3}$. Including transverse diffusion, we get the total efficiency for input field with transverse Gaussian profile

$$\varepsilon_{tot} = e^{-4Dk_i^2 t_{in}/3} \sqrt{\alpha} \frac{1}{1 + 4D(t_H + 2t_{in})/a^2} \quad (25)$$

The efficiency can be improved further by choosing a larger transverse width a , i.e, the effects of transverse diffusion will be reduced by using a smooth field in the transverse direction.

We note that the circumstances in which a GEM will be useful are those for which all dephasing, including that due to diffusion, is small. In this limit, a useful approximate expression for the GEM efficiency is given by

$$\varepsilon_{tot} \simeq 1 - \frac{4Dk_i^2 t_{in}}{3} - \frac{Dt_H \eta^2 t_p^2}{2} - \frac{4D(t_H + 2t_{in})}{a^2}, \quad (26)$$

as the inefficiencies arising from each diffusive process considered above add together.

Experimental considerations give estimates of the achievable GEM efficiency. In particular, to ensure the bandwidth of the memory is large enough to absorb the input field, we require $|\eta t_p| > \frac{1}{L}$, and $t_{in} > t_p$ to ensure that the whole pulse enters the medium during the write-in process, also $|k_i| > \frac{1}{L}$ is required to satisfy $k_H = 0$. So

$$\begin{aligned} \varepsilon_{tot} &\lesssim 1 - \frac{4Dk_i^2 t_p}{3} - \frac{Dt_H}{2L^2} - \frac{4D(t_H + 2t_p)}{a^2} \\ &\lesssim 1 - \frac{4Dt_p}{3L^2} - \frac{Dt_H}{2L^2} - \frac{4D(t_H + 2t_p)}{a^2} \end{aligned} \quad (27)$$

This gives a reasonable upper bound on the GEM efficiency, given the pulse duration $2t_p$, the hold time t_H , and the vapour length L and beam width a .

Experimental considerations: In experiments reported in [14, 21], Rb⁸⁷ atoms were used. Typical system parameters are $\omega_0 = 2\pi \cdot 377.10746$ THz, $\omega_0 - \omega_c = 2\pi \cdot 6.8$ GHz, $\Delta = -2\pi \cdot 1.5$ GHz, $\Omega_c \simeq 2\pi \cdot 20$ MHz, $g \simeq 2\pi \cdot 4.5$ Hz, $t_p = 1\mu\text{s}$, $a \simeq 1.45$ mm, $2L = 0.2$ m, $\eta \simeq -2\pi \cdot 10$ MHz/m, $N \simeq 0.5 \times 10^{18} \text{ m}^{-3}$ [14, 21, 22]. The optical depth $|\beta| \simeq 3.8$ is sufficiently large. According to the formula in [23], we have $D \sim 0.004 \text{ m}^2/\text{s}$ for Rubidium atoms in buffer gas [14, 21].

With these parameters, the diffusive decay will be dominated by transverse diffusion. For example, for $t_{in} = 5\mu\text{s}$ and $t_H = 0$, the maximum achievable efficiency is $\varepsilon_{tot} \simeq 93\%$ ($\varepsilon_{\perp} \simeq \varepsilon_{tot}$, $\varepsilon_H = 1$, $\varepsilon_W \simeq 1$).

We examine the input of the (1,1) Hermite-Gaussian mode $f_{in}(x, y, t) \propto xy e^{-(x^2+y^2)/a^2}$ as an example of a higher order Hermite-Gaussian mode transverse profile. From Eqs. (18, 20), we have $\varepsilon_{\perp} = (\frac{1}{1+\tau_{\perp}})^3$, and the longitudinal diffusion effects are the same as the Gaussian profile

(i.e. the (0,0) Hermite-Gaussian mode). Thus, for diffusive decays, we have

$$\frac{\varepsilon_{(11)}}{\varepsilon_{(00)}} \propto \left(\frac{1}{1+\tau_{\perp}}\right)^2 \quad (28)$$

where $\varepsilon_{(ij)}$ is the read-out efficiency for (ij) Hermite-Gaussian mode. We find that the efficiency decays faster for higher order modes, and the ratio Eq. (28) decreases when the storage time increases. This is in agreement with experimental investigations [21].

E. Output beam width

After some storage time, transverse diffusion will tend to smear the spin wave density in the radial direction. Intuitively, we would expect this to lead to a spatially wider output beam than would be the case in the absence of diffusion.

This is certainly the case when the control field is radially uniform. To see this, we define the intensity distribution for the read-out signal as

$$I(r_{\perp}) = \int |f_{out}(r_{\perp}, t_H + t)|^2 dt. \quad (29)$$

We suppose that the control field is turned off during the hold time, $[0, t_H]$ to avoid control field-induced scattering, and that the gradient is always on and flipped at $t = 0.5t_H$. Also for typical experimental parameters, the effects of longitudinal diffusion is very weak, so we focus on transverse diffusion. We solve the Maxwell-Bloch equation using the same method as before. For a signal with a Gaussian transverse profile, we find that

$$I(r_{\perp}) \propto e^{r_{\perp}^2/[a^2+4D(2t_{in}+t_H)]}. \quad (30)$$

with $r_{\perp}^2 = x^2 + y^2$. Defining $w_{r_{\perp}}$ as the width of the output field, we have

$$w_{r_{\perp}}^2 = \frac{a^2}{4} + D(2t_{in} + t_H), \quad (31)$$

which increases linearly with storage time (Fig. 9), at a rate determined by the diffusion coefficient.

Somewhat surprisingly, the experimentally measured rate of expansion of the read-out signal is smaller than that expected from atomic diffusion by a factor of 2 to 3 [21]. One possible explanation for this is the signal diffraction as suggested in [21], diffusion leads to a beam with reduced divergence and the measurement is taken downstream. However in this experiment the scale of experimental setup is much smaller than the Rayleigh range, so the diffraction effect is too small to explain the observed discrepancy.

Instead, we find that the anomalously narrow output beam width can be explained by considering the control field with realistic transverse Gaussian profile. This leads to a transverse variation in the phase of the spin

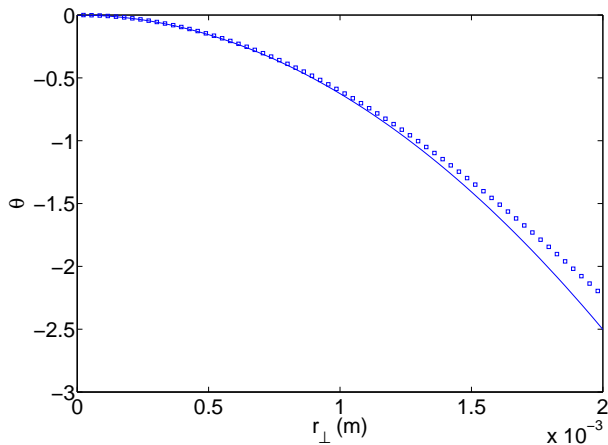


FIG. 7. The extra phase θ for control field with Gaussian profile. Points are numerical results using typical parameters given in the main text, and the curve is the approximate expression in Eq. (32).

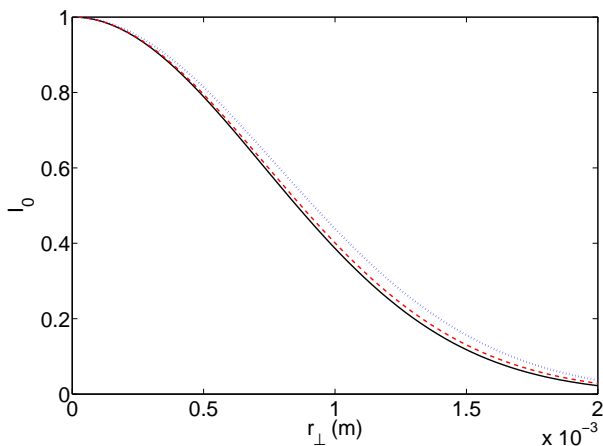


FIG. 8. (Color online) The intensity distribution for the read-out signal with $t_H = 16 \mu\text{s}$. To see the expansion clearly, we have renormalized the maximum of $I(r_\perp)$ to 1, and I_0 is the renormalized intensity distribution. The black solid curve is input signal, the blue dotted one is the read-out signal for homogeneous control field, and the red dashed is read-out signal for control field with Gaussian profile.

wave, which, under the influence of diffusion leads to lower emission efficiency in the wings of the spin wave.

To analyse this effect quantitatively, we consider a Gaussian transverse variation in the control field, $\Omega_c(r_\perp) = \Omega e^{-r_\perp^2/w_c^2}$, with beam waist w_c . Then the two-photon detuning, δ , and the optical depth becomes r_\perp dependent.

From our solution for the spin wave [see Appendix A, Eq. (37)], we find that the inhomogeneity of the control field intensity will introduce a transverse variation in δ , which leads to a transverse dependence in the phase of the spin wave. Likewise, the transverse variation in the optical depth leads to a radially-dependent longitudinal shift in the spin wave $\sigma_{12}(\mathbf{r}, t)$. In combination, these

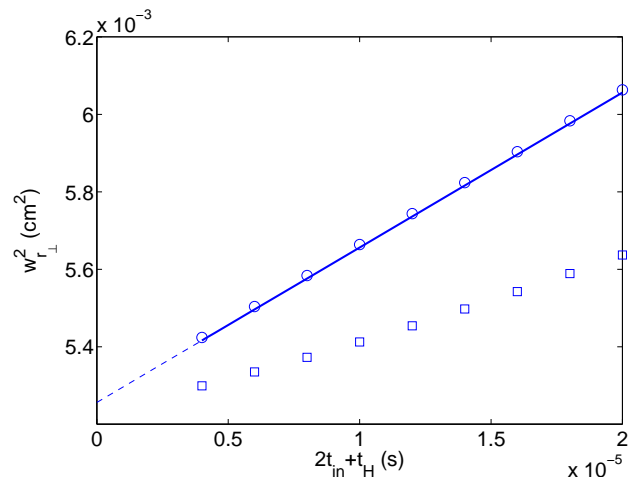


FIG. 9. Expansion of the read-out signal. Circles are numerical results for homogeneous control field. Squares are numerical results for control field with Gaussian profile, the solid line is Eq. (31) for homogeneous control field.

give rise to a radially dependent phase on the spin wave, $e^{i\theta(r_\perp)}$, with the effect of the control field typically being dominant. We compare solutions for this inhomogeneous control field with solutions for the homogeneous control field to obtain the phase difference $\theta(r_\perp)$ during hold time. Typically, the width of the control field, w_c , is much larger than the width of the signal field, a , so $\theta(r_\perp)$ is approximately quadratic in r_\perp/w_c :

$$\theta(r_\perp) = \left[-\frac{2\Omega^2 t_{in}}{\Delta} + 2\beta \ln \left(\left| \frac{\eta L t_{in}}{\beta} + 1 \right| \right) + 2\beta \left(1 - \frac{\Omega^2}{\Delta \eta L} \right) \left(\frac{\beta}{\eta L t_{in} + \beta} + \frac{z}{L} \right) \right] \frac{r_\perp^2}{w_c^2}, \quad (32)$$

where β is the optical depth corresponding to Ω . Because of this quadratic phase variation across the spin wave, diffusion acts to wash out the spin-wave coherence more quickly at larger radius, so the read-out efficiency is suppressed at larger r_\perp . This will tend to reduce the apparent width of the emitted read-out signal.

Experimental considerations: In the experimental results reported in [21], $w_c \simeq 3 \text{ mm}$, and $t_{in} \simeq 2 \mu\text{s}$. Using these parameters, Fig. 7 shows the transverse variation in the phase of the spin-wave at $(z = 0, t = 0.5t_H)$ in the absence of diffusion. When diffusion is introduced, this transverse phase variation is smeared out, leading to reduced read-out efficiency in the wings of the spin-wave. Figure 8 compares the numerical results for the expansion of the read-out signal after a specific hold time, $t_H = 16 \mu\text{s}$, with a homogeneous control field (dotted, blue) and with a spatially varying control field (dashed, red), assuming the diffusion rate $D = 0.004 \text{ m}^2/\text{s}$. Figure 9 shows the variation in the width of the output field as a function of hold time. We see that the expansion is slowed for a control field with Gaussian profile (squares), compared to the case of a uniform control field (circles).

Importantly, this corresponds to a reduction of the beam width expansion-rate by a factor of 2. The apparent diffusion rate extracted from this slower expansion rate is $D_{eff} \simeq 0.002 \text{ m}^2/\text{s}$. This is quantitatively in agreement with the observations in [21].

V. SUMMARY

We have studied the effects of diffusion on the efficiency of the Λ -gradient echo memory, both numerically and analytically. We find that the efficiency is dependent on the spatial frequencies k for both longitude diffusion and transverse diffusion: higher k leads to more pronounced diffusive effects, and reduced efficiency, as expected. We show that the storage efficiency can be improved by appropriate choice of the gradient during the hold phase.

We established a mechanism by which the rate of expansion of the transverse width of the beam is reduced, compared to the naive expectation of diffusive effects. This mechanism arises from the effects of diffusion on the transverse variation in the spin wave phase. We showed that with an experimentally reasonable choice of param-

eters, the magnitude of this effect is the same as that observed in recent experiments. When the density of the buffer gas is increased, the collision rate increases, leading to a smaller diffusion rate. However, this will lead to collision-induced dephasing, which will dominate at sufficiently high buffer gas pressures. This implies a trade off between diffusion- and collision-induced dephasing. This will be the subject of future research.

ACKNOWLEDGMENTS

J. Hope and B. Hillman thank M. Hosseini, D. Higginbottom, O. Pinel and B. Buchler for helpful discussions of the modelling and experiments. J. Hope was supported by the ARC Future Fellowship Scheme. X.-W. Luo thanks G. J. Milburn for helpful discussions, and gratefully acknowledges the National Natural Science Foundation of China (Grants No. 11174270), the National Basic Research Program of China (Grants No. 2011CB921204), CAS for financial support, and The University of Queensland for kind hospitality.

-
- [1] L.M. Duan, M. Lukin, I. Cirac, and P. Zoller. Long-distance quantum communication with atomic ensembles and linear optics. *Arxiv preprint quant-ph/0105105*, 2001.
 - [2] E. Knill, R. Laflamme, G.J. Milburn, et al. A scheme for efficient quantum computation with linear optics. *nature*, 409(6816):46–52, 2001.
 - [3] M. Fleischhauer, A. Imamoglu, and J.P. Marangos. Electromagnetically induced transparency: Optics in coherent media. *Reviews of Modern Physics*, 77(2):633, 2005.
 - [4] M. Fleischhauer and MD Lukin. Dark-state polaritons in electromagnetically induced transparency. *Physical review letters*, 84(22):5094–5097, 2000.
 - [5] J. Nunn, IA Walmsley, MG Raymer, K. Surmacz, FC Waldermann, Z. Wang, and D. Jaksch. Modematching an optical quantum memory. *Arxiv preprint quant-ph/0603268*, 2006.
 - [6] J. Nunn, IA Walmsley, MG Raymer, K. Surmacz, FC Waldermann, Z. Wang, and D. Jaksch. Mapping broadband single-photon wave packets into an atomic memory. *Physical Review A*, 75(1):011401, 2007.
 - [7] B. Kraus, W. Tittel, N. Gisin, M. Nilsson, S. Kröll, and JI Cirac. Quantum memory for nonstationary light fields based on controlled reversible inhomogeneous broadening. *Physical Review A*, 73(2):020302, 2006.
 - [8] N. Sangouard, C. Simon, M. Afzelius, and N. Gisin. Analysis of a quantum memory for photons based on controlled reversible inhomogeneous broadening. *Physical Review A*, 75(3):032327, 2007.
 - [9] M. Afzelius, C. Simon, H. De Riedmatten, and N. Gisin. Multimode quantum memory based on atomic frequency combs. *Physical Review A*, 79(5):052329, 2009.
 - [10] G. Hetet, JJ Longdell, AL Alexander, PK Lam, and MJ Sellars. Gradient echo quantum memory for light using two-level atoms. *Arxiv preprint quant-ph/0612169*, 2006.
 - [11] G. Hetet, JJ Longdell, AL Alexander, P.K. Lam, and MJ Sellars. Electro-optic quantum memory for light using two-level atoms. *Physical review letters*, 100(2):23601, 2008.
 - [12] G. Hétet. *Quantum memories for continuous variable states of light in atomic ensembles*. PhD thesis, Australian National University, 2008.
 - [13] A.I. Lvovsky, B.C. Sanders, and W. Tittel. Optical quantum memory. *Nature Photonics*, 3(12):706–714, 2009.
 - [14] M. Hosseini, BM Sparkes, G. Campbell, PK Lam, and BC Buchler. High efficiency coherent optical memory with warm rubidium vapour. *Nature communications*, 2:174, 2011.
 - [15] O. Firstenberg, M. Shuker, R. Pugatch, DR Fredkin, N. Davidson, and A. Ron. Theory of thermal motion in electromagnetically induced transparency: Effects of diffusion, doppler broadening, and dicke and ramsey narrowing. *Physical Review A*, 77(4):043830, 2008.
 - [16] O. Firstenberg, M. Shuker, N. Davidson, and A. Ron. Elimination of the diffraction of arbitrary images imprinted on slow light. *Physical review letters*, 102(4):43601, 2009.
 - [17] O. Firstenberg, P. London, D. Yankelev, R. Pugatch, M. Shuker, and N. Davidson. Self-similar modes of coherent diffusion. *Physical review letters*, 105(18):183602, 2010.
 - [18] Daniel F Walls and Gerard J Milburn. *Quantum optics*. Springer, 2008.
 - [19] TM Stace and AN Luiten. Theory of spectroscopy in an optically pumped effusive vapor. *Physical Review A*, 81(3):033848, 2010.

- [20] Graham R. Dennis, Joseph J. Hope, and Mattias T. Johnsson. XMDS2: Fast, scalable simulation of coupled stochastic partial differential equations. *Computer Physics Communications*, 184(1):201–208, 2013.
- [21] D.B. Higginbottom, B.M. Sparkes, M. Rancic, O. Pinel, M. Hosseini, P.K. Lam, and B.C. Buchler. Spatial-mode storage in a gradient-echo memory. *Physical Review A*, 86(2):023801, 2012.
- [22] D.A. Steck. Rubidium 87 d line data. *Los Alamos National Laboratory*, 2001.
- [23] W. Happer. Optical pumping. *Reviews of Modern Physics*, 44:169–249, 1972.

APPENDIX A

The Maxwell-Bloch equation for the 1-dimensional model is

$$\begin{aligned} \dot{\sigma}_{12}(z, t) &= i \frac{g\Omega_c}{\Delta} e^{i(k_0 - k_c)z} E(z, t) \\ &\quad - i\delta(z, t)\sigma_{12}(z, t) + D\nabla_z^2 \sigma_{12}(z, t), \\ \frac{\partial}{\partial z} E(z, t) &= i \frac{gN\Omega_c}{c\Delta} e^{-i(k_0 - k_c)z} \sigma_{12}(z, t) \\ &\quad + i \frac{g^2 N}{c\Delta} E(z, t). \end{aligned} \quad (33)$$

To find the solution during $[-t_0, 0]$, we first solve the equation without diffusion, then introduce the diffusion effects to our solutions.

When $D = 0$, we can make transformation

$$\begin{aligned} \tilde{\sigma}_{12}(z, t) &= e^{-i \frac{g^2 N}{c\Delta} z} e^{-i(k_0 - k_c)z} \sigma_{12}(z, t), \\ \tilde{E}(z, t) &= e^{-i \frac{g^2 N}{c\Delta} z} E(z, t), \end{aligned} \quad (34)$$

and get the new equations

$$\begin{aligned} \partial_z \tilde{E}(z, t) &= i \frac{g_{eff} N}{c} \tilde{\sigma}_{12}(z, t), \\ \partial_t \tilde{\sigma}_{12}(z, t) &= -i\eta z \tilde{\sigma}_{12}(z, t) + i g_{eff} \tilde{E}(z, t) \end{aligned} \quad (35)$$

where $g_{eff} = g\Omega_c/\Delta$. Following the method given in [10], and using the boundary conditions $\tilde{\sigma}_{12}(z, t \rightarrow -\infty) = 0$ and $\tilde{E}(z = -L, t < 0) = \tilde{f}_{in}(t)$, we integrate the first equation and substitute it in the second one. Making use of Fourier transformation, we find

$$\tilde{E}(k, t) = \tilde{f}_{in}\left(\frac{k}{\eta} + \frac{\beta}{\eta L} + t\right) \left|\frac{k}{\eta}\right|^{-i\beta-1} G(\eta, \beta, L), \quad (36)$$

and

$$G(\eta, \beta, L) = \frac{1}{\eta} \beta e^{-\pi|\beta|/2} \sinh(\pi|\beta|) |\eta L|^{-i\beta} \Gamma(i\beta),$$

where $\tilde{E}(k, t) = \int \tilde{E}(z, t) e^{-ikz} dz$, $\beta = \frac{g_{eff}^2 N}{\eta c}$ is the optical depth and we assume β is sufficiently large, $\Gamma(i\beta)$ is the Gamma Function, $\tilde{f}_{in}(t) = f_{in}(t) e^{i \frac{g^2 N}{c\Delta} L}$ is the input pulse. According to the Maxwell-Bloch equations, we have $\tilde{\sigma}_{12}(k, t) = \frac{k \cdot c}{g_{eff} N} \tilde{E}(k, t)$.

We transform $\tilde{\sigma}_{12}(k, t)$ back to $\sigma_{12}(k, t)$,

$$\begin{aligned} \sigma_{12}(k, t) &= f_{in}\left(\frac{k - k_i}{\eta} + t\right) e^{i \frac{g^2 N}{c\Delta} L} \\ &\quad \times \left|\frac{k - k_i}{\eta} - \frac{\beta}{\eta L}\right|^{-i\beta} \text{sgn}\left(\frac{k - k_i}{\eta} - \frac{\beta}{\eta L}\right) \frac{c}{g_{eff} N} G \end{aligned} \quad (37)$$

with $k_i = \frac{g^2 N}{c\Delta} + k_0 - k_c - \frac{\beta}{L}$.

Now we introduce the diffusion, for the short time interval $[t, t + \Delta t]$, diffusion will cause a decay $e^{-Dk^2 \Delta t}$ to

$\sigma(k, t)$, or equally, there will be a decay $e^{-Dk^2\Delta t}$ on the signal $f_{in}(t')$ with $k = k_i - \eta(t - t')$. So the total decay during the write-in process for $f_{in}(t')$ is

$$e^{-D \int_{t'}^0 (k_i - \eta(t - t'))^2 dt} = e^{-\frac{D}{3\eta}(k_i^3 - (k_i + \eta t')^3)}.$$

Thus, the solution for σ_{12} at $t = 0$ is

$$\begin{aligned} \sigma_{12}(k, 0) &= e^{-\frac{D}{3\eta}(k_i^3 - k^3)} f_{in}\left(\frac{k - k_i}{\eta}\right) e^{i\frac{g^2 N}{c\Delta} L} \\ &\times \left| \frac{k - k_i}{\eta} - \frac{\beta}{\eta L} \right|^{-i\beta} \text{sgn}\left(\frac{k - k_i}{\eta} - \frac{\beta}{\eta L}\right) \frac{c}{g_{eff} N} G. \end{aligned} \quad (38)$$

We have assumed that the bandwidth of the memory is larger than the bandwidth of the input signal, $|\eta L| \gg \Delta\omega_s$, and the optical depth is sufficient large, $\beta \gtrsim 1$. The signal will be absorbed near $z = 0$, and $\sigma_{12}(z, 0)$ and $E(z, 0)$ is nonzero only near $z = 0$, so we can treat L as infinity during $[0, t_H]$. Also notice that, the gradient is turned off during $[0, t_H]$, and the spatial frequency k will hold its value.

To get the solution in $[0, t_H]$, we solve Eq. (33) with initial condition $\sigma_{12}(k, t = 0)$ for σ_{12} and open boundary condition for E . In k space, we find

$$\sigma_{12}(k, t_H) = e^{-Dk^2 t} e^{i\frac{g_{eff}^2 N}{c} \frac{1}{k-k} t_H} \sigma_{12}(k, 0) \quad (39)$$

where $\bar{k} = \frac{g^2 N}{c\Delta} + k_0 - k_c$. Notice that $\sigma_{12}(k, t_H)$ get a phase $e^{i\frac{g_{eff}^2 N}{c} \frac{1}{k-k} t_H}$, so the group velocity for $\sigma_{12}(z, t)$ is $v_g(k) = \frac{g_{eff}^2 N}{c(k-k)^2}$. If the memory broadening $|\eta L|$ is not much larger than the signal pulse bandwidth, the spin wave $\sigma_{12}(z, t)$ will be nonzero near the ensemble boundary. Then the spin wave will propagate to the boundary and be reflected, this may ruin the spin wave coherence near the boundary and lower the memory efficiency. One way to avoid this effect is turning off the control field during storage, which makes the effective coupling $g_{eff} = 0$, and the group velocity $v_g = 0$.

To find the values for σ_{12} and E in the duration $[t_H, t_H + t_0]$, one needs to solve a modified version of Eq. (33) where the sign of $i\eta z$ is reversed. We follow the method given in [10], propagate these equation backwards with final conditions $E(z = L, t > t_H) = f_{out}(t), \sigma_{12}(z, t \rightarrow \infty) = 0$. Similar to the write-in process, at time t_H , we have

$$\begin{aligned} \sigma_{12}(k, t_H) &= e^{\frac{D}{3\eta}(k_i^3 - k^3)} f_{out}\left(t_H + \frac{k - k_i}{-\eta}\right) e^{-i\frac{g^2 N}{c\Delta} L} \\ &\times \left| \frac{k - k_i}{\eta} - \frac{\beta}{\eta L} \right|^{-i\beta} \text{sgn}\left(\frac{k - k_i}{\eta} - \frac{\beta}{\eta L}\right) \frac{c}{g_{eff} N} G^*. \end{aligned} \quad (40)$$

By matching the two solutions for σ_{12} at t_H Eqs. (39), (40), we get

$$f_{out}(t_H + t) = d_W(t) d_H d_R(t) f_{in}(-t) \bar{G} \quad (41)$$

where

$$\bar{G} = |\eta L \left(t + \frac{\beta}{\eta L} \right)|^{-i2\beta} e^{i\frac{2Lg^2 N}{c\Delta}} e^{-i\frac{g_{eff}^2 N}{c\eta \left(t + \frac{\beta}{\eta L} \right)} t_H} \Gamma(i\beta) / \Gamma(-i\beta)$$

is a phase factor, $d_W(t) = e^{-\frac{D}{3\eta}(k_i^3 - (k_i - \eta t)^3)}$, $d_H = e^{-D(k_i - \eta t)^2 t_H}$ and $d_R(t) = e^{-\frac{D}{3\eta}(k_i^3 - (k_i - \eta t)^3)}$ are the diffusion decays for the write-in process $[-t_0, 0]$, storage time $[0, t_H]$ and read-out process $[t_H, t_H + t_0]$ respectively.

APPENDIX B

The Maxwell-Bloch equation for the 3-dimensional model is

$$\begin{aligned} \dot{\sigma}_{12}(\mathbf{r}, t) &= i\frac{g\Omega_c}{\Delta} e^{i(k_0 - k_c)z} E(\mathbf{r}, t) \\ &\quad - (i\eta z)\sigma_{12}(\mathbf{r}, t) + D\nabla^2 \sigma_{12}(\mathbf{r}, t), \\ \frac{\partial}{\partial z} E(\mathbf{r}, t) &= i\frac{gN\Omega_c}{c\Delta} e^{-i(k_0 - k_c)z} \sigma_{12}(\mathbf{r}, t) \\ &\quad + i\frac{g^2 N}{c\Delta} E(\mathbf{r}, t). \end{aligned} \quad (42)$$

To solve these equations, we first transform transverse coordinates x, y to Fourier space k_x, k_y ,

$$\begin{aligned} \dot{\sigma}_{12}(k_x, k_y, z, t) &= - (i\eta z + \gamma_k)\sigma_{12}(k_x, k_y, z, t) \\ &\quad + i\frac{g\Omega_c}{\Delta} e^{i(k_0 - k_c)z} E(k_x, k_y, z, t) \\ &\quad + D\nabla_z^2 \sigma_{12}(k_x, k_y, z, t), \\ \frac{\partial}{\partial z} E(k_x, k_y, z, t) &= i\frac{gN\Omega_c}{c\Delta} e^{-i(k_0 - k_c)z} \sigma_{12}(k_x, k_y, z, t) \\ &\quad + i\frac{g^2 N}{c\Delta} E(k_x, k_y, z, t), \end{aligned} \quad (43)$$

where $\gamma_k = D(k_x^2 + k_y^2)$. Now we make the following transformation:

$$\begin{aligned} \bar{\sigma}_{12}(k_x, k_y, z, t) &= e^{\gamma_k t} \sigma_{12}(k_x, k_y, z, t), \\ \bar{E}(k_x, k_y, z, t) &= e^{\gamma_k t} E(k_x, k_y, z, t), \end{aligned} \quad (44)$$

then we have

$$\begin{aligned} \dot{\bar{\sigma}}_{12}(k_x, k_y, z, t) &= - (i\eta z)\bar{\sigma}_{12}(k_x, k_y, z, t) \\ &\quad + i\frac{g\Omega_c}{\Delta} e^{i(k_0 - k_c)z} \bar{E}(k_x, k_y, z, t) \\ &\quad + D\nabla_z^2 \bar{\sigma}_{12}(k_x, k_y, z, t), \\ \frac{\partial}{\partial z} \bar{E}(k_x, k_y, z, t) &= i\frac{gN\Omega_c}{c\Delta} e^{-i(k_0 - k_c)z} \bar{\sigma}_{12}(k_x, k_y, z, t) \\ &\quad + i\frac{g^2 N}{c\Delta} \bar{E}(k_x, k_y, z, t). \end{aligned} \quad (45)$$

These are actually quasi-1D equations, so we can solve these equations by the method we used before, and the output field is:

$$\bar{f}_{out}(k_x, k_y, t_H + t) = d_W(t) d_H d_R(t) \bar{f}_{in}(k_x, k_y, -t) \bar{G}.$$

We transform back to $f_{out}(k_x, k_y, t_H + t)$, and get

$$f_{out}(k_x, k_y, t_H + t) = d_W(t) d_H d_R(t) \times d_{\perp}(t) f_{in}(k_x, k_y, -t) \bar{G}, \quad (46)$$

where $d_{\perp}(t) = e^{-2\gamma_{\kappa} t} e^{-\gamma_{\kappa} t_H}$ is the transverse diffusion decay.